



SPE 55628

Mechanism for Gel Propagation Through Fractures

R. S. Seright, SPE, New Mexico Petroleum Recovery Research Center

Copyright 1999, Society of Petroleum Engineers Inc.

This paper was prepared for presentation at the 1999 SPE Rocky Mountain Regional Meeting held in Gillette, Wyoming, 15–18 May 1999.

This paper was selected for presentation by an SPE Program Committee following review of information contained in an abstract submitted by the author(s). Contents of the paper, as presented, have not been reviewed by the Society of Petroleum Engineers and are subject to correction by the author(s). The material, as presented, does not necessarily reflect any position of the Society of Petroleum Engineers, its officers, or members. Papers presented at SPE meetings are subject to publication review by Editorial Committees of the Society of Petroleum Engineers. Electronic reproduction, distribution, or storage of any part of this paper for commercial purposes without the written consent of the Society of Petroleum Engineers is prohibited. Permission to reproduce in print is restricted to an abstract of not more than 300 words; illustrations may not be copied. The abstract must contain conspicuous acknowledgment of where and by whom the paper was presented. Write Librarian, SPE, P.O. Box 833836, Richardson, TX 75083-3836, U.S.A., fax 01-972-952-9435.

Abstract

Many conformance control treatments rely on the ability of gels to extrude through fractures during the placement process. This paper describes an experimental investigation of the mechanism for propagation of a Cr(III)-acetate-HPAM gel through fractures. When large volumes of this gel were extruded through a fracture, progressive plugging (i.e., continuously increasing pressure gradients) was not observed. Effluent from the fracture had the same appearance and a similar composition as those for the injected gel, even though a concentrated, immobile gel formed in the fracture. The concentrated gel formed when water leaked off from the gel along the length of the fracture. The driving force for gel dehydration (and water leakoff) was the pressure difference between the fracture and the adjacent porous rock. During gel extrusion through a fracture of a given width, the pressure gradients along the fracture and the dehydration factors were the same for fractures in 650-md sandstone as in 50-md sandstone and 1.5-md limestone. A simple model was developed that accounted for many of the experimental results.

Introduction

Some of the most successful treatments to reduce water and gas channeling in reservoirs used large volumes of gel that extruded through fractures during the placement process.¹⁻⁴ A need exists to determine how much gel should be injected in a given application and where that gel distributes in a fractured reservoir. These parameters depend critically on the properties of gels in fractures. Therefore, we have a research program to determine these properties. In previous work,⁵⁻⁸ we demonstrated that a minimum pressure gradient was required to extrude a given gel through a fracture. Once this minimum pressure gradient was exceeded, the pressure gradient during

gel extrusion was insensitive to the flow rate. This behavior was attributed to a strong “slip” effect exhibited by the gel.^{5,6,8} In particular, when an element of gel extruded through a fracture, it moved as a plug, with a flow discontinuity occurring between the gel plug and the fracture faces. In other words, little or no viscous dissipation of energy occurred within the moving gel plug.

The pressure gradient required for gel extrusion varied inversely with the square of fracture width (**Fig. 1**). We also found that gels can concentrate (dehydrate) during extrusion through fractures. Depending on fracture width (see **Fig. 2**), this dehydration effect can significantly retard gel propagation (e.g., by factors up to 50). Figs. 1 and 2 apply to a one-day-old Cr(III)-acetate-HPAM gel [0.5% Alcoflood 935 HPAM, 0.0417% Cr(III) acetate] at 41°C. (Ref. 5 provides details of the experiments.)

The objective of our current work is to understand the mechanism for gel extrusion and dehydration in fractures. With this understanding, we ultimately hope to predict conditions, gel compositions, and gel volumes that provide the optimum gel placement in fractured reservoirs. The specific questions addressed in this paper are:

1. If a large volume of gel is injected into a fracture, will pressure gradients stabilize or continuously increase?
2. During gel extrusion, how do pressure gradients in the porous rock compare to those in the fracture?
3. What is the composition of fluids that flow in the fracture versus the porous rock?
4. Where and how does gel dehydrate during extrusion through a fracture?
5. During extrusion, does the performance of the gel depend on the permeability of the porous rock?
6. If a fracture contains proppant, what pressure gradient and degree of gel dehydration are observed during gel extrusion?

Experimental

To probe the mechanism for gel propagation and dehydration, an experiment was performed where a Cr(III)-acetate-HPAM gel was extruded through a four-ft-long fractured core. The core (see **Fig. 3**) was prepared from 650-md Berea sandstone, fractured lengthwise, and cast in epoxy using our standard method.⁵⁻⁸ The core height and width were both 1.5 in. (3.81 cm). The fracture height was also 1.5 in., and the fracture was

oriented vertically during the experiments. The effective average fracture width was 0.04 in. (0.1 cm), and the average fracture conductivity was 277 darcy-ft. The fracture volume was 2.84 in.³ (46.5 cm³), and the core pore volume was 24.1 in.³ (395 cm³). Four equally spaced internal taps were positioned to measure pressures along the length of the fracture. Four equally spaced internal taps also were placed to measure pressures along the length of the porous rock. These sets of taps divided the core into five sections of equal length. One additional internal pressure tap was placed to measure pressure in the matrix just after the inlet sand face. A special fitting (**Fig. 4**) was epoxied to the core outlet to segregate the effluent from the fracture and that from the porous rock. Before gel injection, the fractured core was saturated with brine and characterized using tracer studies and flow measurements.⁵⁻⁸

Our experiments used an aqueous gel that contained 0.5% Allied Colloids Alcoflood 935 HPAM (molecular weight $\approx 5 \times 10^6$ daltons; degree of hydrolysis 5% to 10%), 0.0417% Cr(III) acetate, 1% NaCl, and 0.1% CaCl₂ at pH=6. All experiments were performed at 41°C (105°F). The gelant formulations were aged at 41°C for 24 hours (5 times the gelation time) before injection into a fractured core.

Results

Pressure Gradients in the Fracture. We extruded 80 fracture volumes (226 in.³ or 3,700 cm³) of one-day-old Cr(III)-acetate-HPAM gel through the 4-ft-long fractured core using an injection rate of 12.2 in.³/hr (200 cm³/hr). **Fig. 5** shows the pressure gradients in the fracture for the five fracture sections during gel injection. At the end of gel injection, the average pressure gradient in the fracture was 28 psi/ft for the first three fracture sections and 50 psi/ft in the last two fracture sections. This result suggests that the last two fracture sections were slightly narrower and less conductive than the first three fracture sections. In all sections, the pressure gradients were reasonably stable during the last 60 fracture volumes of gel injection. Thus, gel injection did not exhibit progressive plugging (i.e., continuously increasing pressure gradients) in any part of the fracture.

Pressure Gradients in the Porous Rock. During gel injection, pressure gradients in the porous rock are shown in **Fig. 6** for the five sections of the core. These pressure gradients were typically between 0.2 and 1.0 psi/ft—much lower than the values observed in the fracture. For a given section, the onset of a pressure response occurred at the same injection volume for both the fracture pressure gradients and the matrix pressure gradients (compare **Figs. 5** and **6**).

Produced Fluids. As mentioned earlier, a special outlet fitting segregated the effluent from the fracture and that from the porous rock. **Fig. 7** plots the fraction of the effluent that was produced from the fracture versus from the porous rock. During the first 15 fracture volumes of gel injection, virtually 100% of the flow occurred in the fracture. This result was

expected. Before gel injection, the calculated flow capacity of the fracture was 3,400 times greater than the flow capacity of the porous rock. Gel arrived at the fracture outlet after injecting 15 fracture volumes of gel. Coincident with gel arrival, flow from the fracture abruptly stopped for a period of about 2 fracture volumes of gel injection. (So, 100% of the effluent was produced from the matrix during this time.) Subsequently, the fraction of flow from the fracture increased, while flow from the porous rock decreased. After injecting 80 fracture volumes of gel, flow from the fracture accounted for 65% of the total flow, while flow from the matrix accounted for 35% of the total flow.

The physical appearance of the gel from the fracture outlet was the same as that of the injected gel. Also, the composition of the gel from the fracture outlet was similar to that of the injected gel. Chromium concentrations were measured using atomic absorption spectroscopy (by the New Mexico BMMR Chemistry Laboratory), and HPAM concentrations were determined using total organic carbon analysis (Shimadzu TOC-5050A). The chromium and HPAM concentrations are plotted in **Fig. 8** for effluent samples from the fracture and the matrix. This figure confirms that the fracture provided the only conduit for the gel. After gel breakthrough, the chromium concentration averaged 1.17 times that of the injected gel, while the polymer concentration averaged 1.35 times that of the injected gel. Chromium and polymer concentrations for the matrix effluent were negligible.

Gel Composition in the Fracture. After gel injection, the fracture was opened to reveal a rubbery gel that completely filled the fracture. This gel (after 80 fracture volumes of gel injection) was analyzed for chromium and HPAM as a function of length along the fracture (solid symbols in **Fig. 9**). The chromium and HPAM concentrations in the fracture averaged 28.7 and 26.0 times those for the injected gel, respectively. The gel became somewhat less concentrated with increased distance along the fracture. In the first 25% of the fracture, the gel was about 50% more concentrated than in the final 25% of the fracture.

The open symbols in **Fig. 9** show chromium and HPAM content for gel from a separate, identical experiment, except that only 17 fracture volumes of Cr(III)-acetate-HPAM gel were injected. (Details of this experiment can be found in Ref. 5.) At the end of this experiment, the chromium and HPAM concentrations in the fracture averaged 14.3 and 9.5 times those for the injected gel, respectively. Again, the gel became somewhat less concentrated with increased distance along the fracture. **Fig. 9** suggests that gel in the fracture became more concentrated with increased throughput of the injected gel.

Discussion

Gel Injection Did Not Cause Progressive Plugging. In previous work using 4-ft-long fractured cores, less than 20 fracture volumes of gel were typically injected.⁵⁻⁸ During these experiments, pressure gradients appeared to stabilize along the fracture during gel injection at a fixed flow rate. However, we wondered whether pressure gradients might continuously

increase during injection of larger gel volumes. The results from our new experiment (Fig. 5) diminish this concern.

The pressure behavior in Fig. 5 shows the rate of gel propagation through the fracture. In particular, gel first entered Fracture Sections 2, 3, 4, and 5 after injecting 1.1, 2.7, 5.6, and 11 fracture volumes of gel, respectively. (Fig. 5 also suggests that 0.3 fracture volumes of gel were required before entering Section 1. This result simply reveals the experimental error associated with timing at the start of the coreflood.) Gel was first detected in the effluent from the fracture after injecting 15 fracture volumes of gel. Fig. 10 indicates the rate of gel propagation in the five fracture sections relative to that expected for a displacement with no retardation or dispersion of the gel front in the fracture. In the first fracture section, the rate of gel propagation was about one-fifth that for an unimpeded displacement, while in the fourth and fifth fracture sections, gel propagated at about one-twenty-fifth of the rate for an unimpeded displacement.

Gel That Concentrated Became Immobile. Although gel that remained in the fracture at the end of the experiment was concentrated by factors up to 40 (Fig. 9), the gel that actually propagated through the fracture had a composition similar to that of the injected gel (Fig. 8). This result implies that for the most part, gel that dehydrated in the fracture ceased to propagate. In the next three sections, dehydrated gel will be shown to form as a filter cake on the fracture faces.

Brine Flow in Porous Rock Was Substantial. The pressure gradients shown in Fig. 6 indicate fluid flow in the porous rock during gel injection. That fluid was exclusively brine—based on Figs. 7 and 8 and previous proof that the Cr(III)-acetate-HPAM gel does not flow through porous rock.⁷ Of course, the source of this flow was water that left the gel in the fracture—i.e., water from the gel dehydration process.

The Darcy equation was used to convert the pressure gradients in Fig. 6 to flow rates. (Rock permeability was 650 md, and brine viscosity was 0.67 cp at 41°C.) Since the total injection rate was fixed (at 200 cm³/hr), the matrix flow rates, in turn, were converted to the fraction of total flow that occurred through the rock matrix at any given time. Fig. 11 plots the results of this conversion. For a given position along the core, flow through porous rock did not become significant until the gel front reached that position in the fracture. Shortly after arrival of the gel front in the adjacent fracture, flow in the porous rock rose to a maximum between 35% and 60% of the total flow (i.e., a minimum between 40% and 65% of the total flow occurred in the fracture). Then, the fraction of total fluid flow gradually declined. After injecting 80 fracture volumes of gel, the fraction of flow in the matrix ranged from 0.1 to 0.35.

At any given time, Fig. 11 plots the average fraction of the total flow that occurred in the porous rock in each of the five core sections. For comparison, Fig. 7 plots the measured fraction of total flow (in the matrix versus in the fracture) at a single position—at the outlet of the fractured core. The two data sets were consistent in that at the end of gel injection, the

final fractional flow from the matrix (35%) was the same in Fig. 7 as that in Fig. 11 for the fifth section of the core.

Brine Leakoff Peaked after the Gel Front Passed. Utilizing a mass balance, the data in Fig. 11 was used to determine the leakoff rate through the fracture faces for the different sections of the core. In particular, the flow rate in the matrix of a given core section was the sum of the leakoff from the fracture faces plus the flow rate from the matrix of the previous (upstream) core section. Fig. 12 plots the leakoff rate per unit of fracture face versus the fracture volumes of gel injected for the various sections of the core. Again, the source of the leakoff was water that left the gel in the fracture. The leakoff rates were normalized relative to the largest leakoff rate observed during the experiment (i.e., 1.89×10^{-4} ft³/ft²/min or 9.63×10^{-5} cm³/cm²/s).

For any given section, Fig. 12 demonstrates that the leakoff rate rapidly rose to a maximum and then gradually diminished. A comparison of Figs. 5 and 12 reveals that in all but the first section, the onset of leakoff lagged significantly behind the arrival of the gel front in the fracture. In particular, in each section, the onset of leakoff corresponded very closely to the arrival of the gel front at the beginning of the next (downstream) fracture section. Since each core section was about 10 in. long, the onset of leakoff lagged about 10 in. behind the gel front.

The greatest leakoff rate was observed in the first core section after injecting about one fracture volume of gel. In Fig. 12, this maximum rate was arbitrarily assigned a value of unity. The peak leakoff rates in Sections 2, 3, 4, and 5 were 67%, 56%, 53%, and 54% of this value, respectively. After injecting 80 fracture volumes of gel, the relative leakoff rates varied from 0 (in Section 2) to 0.5 (in Section 5).

Concentrated Gel Formed as a Filter Cake. How does concentrated gel form in the fracture? Fig. 12 provides some insight into this issue. As mentioned earlier, at a given point along the fracture, the onset of leakoff may lag behind the gel front by about 10 in. Of course, gel in the fracture near the front inhibits flow for gel farther upstream. Also, the pressure differences between the fracture and the matrix are greater in the early parts of the fracture than near the gel front. Thus, the upstream gel has a greater tendency to form a filter cake of concentrated gel against the fracture face.

Behind the gel front, Fig. 12 reveals that leakoff occurred and the gel lost water along most of the gel-contacted portion of the fracture. In other words, gel dehydration did not occur all at once when the gel first entered the fracture, nor did it occur exclusively at the gel front. Our results suggest that a filter cake of concentrated gel formed gradually along the length of the fracture. We envision that the gel filter cake formed on the fracture face because of the high-pressure gradient between the fracture and the adjacent matrix.

At a given point in the fracture, Fig. 12 reveals that the leakoff rate gradually decreased after the gel front passed. This result indicates that thicker or more concentrated gel filter cakes accumulated on the fracture faces in the upstream

sections. This suggestion is supported by Fig. 9. Furthermore, in our experience to date,⁵⁻⁸ the concentrated gel completely filled the width of the fracture, no matter how much (or how little) gel was injected. We saw no direct evidence that the filter cake increased in thickness with increased gel throughput. In other words, for most of the gel placement process, the filter cake “grew” (or increasingly inhibited water leakoff) by becoming more concentrated, rather than by increasing in thickness. This suggestion is supported by a comparison of the solid and open data points in Fig. 9. Interestingly, even though the gel became increasingly concentrated with increased throughput, the pressure gradient required for extrusion did not increase during the last 60 fracture volumes of gel injection (Fig. 5).

The leakoff data was used to estimate the average permeability to water for the concentrated gel. Near the end of gel injection, the average permeability of the gel filter cake was 0.3 μd .

Given that gel does not flow into the porous rock,⁷ a mass balance was applied to the data in Fig. 12 to estimate the total weight of chromium and HPAM that remained in the fracture after 80 fracture volumes of gel injection. This calculation was performed for the entire fracture and for each of the five fracture sections. The results were compared with the actual final mass of chromium and HPAM in the fracture, based on the solid symbols in Fig. 9. This comparison revealed that the final chromium mass in the fracture accounted for 92% of the value expected from the leakoff calculation. The final HPAM mass in the fracture accounted for 76% of the value expected from the leakoff calculation. These values apply to the entire core. Individual results for the first, third, and fourth sections of the core were very similar to those for the entire core. For the second core section, the actual chromium and HPAM masses in the fracture were two to three times those expected from the leakoff calculation. For the fifth core section, the actual chromium and HPAM masses in the fracture were 30-45% of those expected from the leakoff calculation. The discrepancies for the second and fifth sections may have been caused by pressure errors during the flow measurements.

The above results indicate that when an element of gel experiences dehydration, most of the chromium and HPAM remain in the fracture. However, a fraction of free chromium and uncrosslinked HPAM may leak off into the porous rock along with the water from the dehydration process. This suggestion was confirmed during a sandpack experiment that is described in the next section. Presumably, in Berea sandstone, the free chromium and uncrosslinked HPAM were retained by the rock, so they were never produced through the matrix. During the experiment, the total amount of brine produced from the matrix was 4.1 core pore volumes (PV). If 76% to 92% of the original HPAM and chromium, respectively, were removed from the brine before entering the rock (as indicated above), the remaining HPAM and chromium in 4.1 PV of brine could easily be removed by retention in the Berea sandstone. Thus, the absence of

chromium and HPAM in the effluent from the matrix was not surprising (Fig. 8).

Pressure Gradients Were High in a Sandpack. Our previous experiments used open fractures, with no proppant. However, many hydraulic fractures contain a proppant, such as coarse sand. In a propped fracture, the gel must extrude through the porous sandpack in the fracture. What pressure gradients and degree of gel dehydration are observed as a gel extrudes through a sandpack? To answer this question, our standard 24-hour-old Cr(III)-acetate-HPAM gel was extruded through an industrial quartz (Ottawa) sandpack. The sandpack was 2.7 ft (82 cm) long and 2.5 in. (6.4 cm) in diameter. Four internal pressure taps were spaced equally along the pack, dividing the pack into five 6.5-in.-long sections. The permeability of the pack was 28 darcys, and the total pore volume was 62.4 in.³ (1,022 cm³). Using a capillary bundle model, the effective average pore size in the pack was estimated to be about 0.006 in. (0.015 cm).

While injecting Cr(III)-acetate-HPAM gel (at 41°C) using an injection rate of 12.2 in.³/hr (200 cm³/hr), the average pressure gradient in the gel-contacted portion of the core was about 200 psi/ft. This value was roughly the pressure gradient observed when extruding this gel through a 0.006-in.-wide fracture (see Fig. 1). Of course, 200 psi/ft is a very high-pressure gradient—raising concern about the feasibility of extruding this gel through a propped fracture.

After injecting one PV of gel, the pressure behavior indicated that the gel front reached 40% of the distance through the sandpack. Although no gel was detected in the effluent from the sandpack, some free (apparently) chromium and uncrosslinked HPAM were found in the effluent. This finding is shown in Fig. 13. The first chromium was detected at 0.85 PV, while the first HPAM was observed at 1.15 PV. After injecting 1.6 PV of gel, the chromium and HPAM concentrations in the effluent reached 28% and 6.6%, respectively, of the concentrations in the original gel. This experiment represents the first time that free chromium and uncrosslinked HPAM were produced from our core experiments significantly before gel was produced. In our previous experiments (e.g., Fig. 8), the chromium, HPAM, and gel fronts arrived at the core outlets simultaneously (through the fractures). In Berea sandstone, any free chromium or HPAM that leaked off with water through the fracture faces were probably retained by the porous rock. However, in the present sandpack experiment, chromium and HPAM retention by quartz was much less than that by Berea sandstone, so these chemicals propagated through the porous medium more readily.

Near the end of gel injection, small samples were collected from each of the four internal taps. Relative to the original gel, the chromium concentrations of these samples were 100%, 100%, 56%, and 49% for the first through fourth internal taps, respectively. The relative HPAM concentrations of these samples were 100%, 88%, 8.3%, and 8.0%, respectively. These results suggest that at the first and second internal taps,

the flowing gel had the same composition as that for the original gel. In contrast, at the third and fourth internal taps, only free chromium and uncrosslinked HPAM were flowing. Interestingly, at the end of the experiment, analysis of gel on the inlet sand face revealed that the gel was concentrated by a factor of about 10. In particular, the chromium was concentrated by a factor of 12, while the HPAM was concentrated by a factor of 9.5.

Flowing Gel May Be Concentrated Slightly. Returning to our earlier fracture experiment, Fig. 7 suggests that after 80 fracture volumes, each new element of injected gel should be concentrated by 35% (because water produced from the matrix stabilized at 35% of the total flow). Figs. 5, 7, and 8 indicate that near the end of the experiment, a steady state was attained. Therefore, some concentrated (dehydrated) gel must propagate through the fracture. Two possibilities are evident. First, the propagating gel may be homogeneous (i.e., with a uniform concentration that was roughly 35% greater than the injected gel). Alternatively, the propagating gel may be a mixture of two components. The injected gel may comprise the dominant component, while a minor component may be very concentrated gel with the composition of the material found in the fracture at the end of the experiment (i.e., gel that was ~27 times more concentrated than the injected gel). In other words, at steady state, we suggest that pressure gradients may be great enough to mobilize a small amount of the dehydrated gel. More work is needed to distinguish between these possibilities.

Rock Permeability Did Not Affect Gel Extrusion. Of course, the extrusion properties of a gel depend on the fracture width (see Figs. 1 and 2). However, does the performance of the gel depend on the permeability of the rock that is adjacent to the fracture? Most of our previous work used fractured 650-md Berea sandstone. Therefore, several extrusion experiments were conducted using fractured 50-md Berea sandstone and 1.5-md Indiana limestone. Details of the experimental procedures can be found in Ref. 5. The pressure gradients required for extrusion are shown by the open symbols in Fig. 1, while the degrees of dehydration experienced by the gel are shown by the open symbols in Fig. 2. These figures demonstrate that the performance of the gel was not sensitive to rock permeability.

To understand this finding, note that gel permeability (typically in the μd range) was always much less than the rock permeability (1.5 md or greater). Therefore, the gel permeability determined the rate at which water (from the dehydration process) entered the rock. The degree of dehydration was affected by the pressure difference between the fracture and the porous rock next to the fracture. In most of our experiments, the flow capacity of the rock was sufficient to rapidly drain any water of dehydration from the gel. (This condition also occurs in virtually all field applications.⁵) Therefore, the pressure in the rock was always quite low, and the pressure difference was fairly high between the fracture

and the adjacent porous rock. For a given position along the fracture, this pressure difference was insensitive to rock permeability, since the pressure gradient in the fracture was determined primarily by fracture width (Fig. 1). Consequently, the degree of gel dehydration was also insensitive to rock permeability. (Incidentally, when performing experiments with 1.5-md limestone, the core must be designed or sized with sufficient flow capacity to adequately drain the water that was dehydrated from the gel. Otherwise, gel dehydration may be underestimated.)

Model for Gel Propagation and Dehydration

The experimental results suggest that gel dehydration occurred because the pressure in the fracture was much greater than that in the porous rock next to the fracture. Since the gel had a finite permeability to water⁹ and since the crosslinked polymer did not penetrate into the porous rock,⁷ water flowed from the gel (in the fracture) into the porous rock. This action increased the average gel concentration in the fracture. For the most part, the concentrated gel was immobile.

At a given point along the fracture, the leakoff rate per unit area of fracture face, u_l , was estimated from the Darcy equation.

$$u_l = 2k_{gel} Dp / (w_f m) \dots\dots\dots (1)$$

In Eq. 1, k_{gel} is gel permeability to water, m is water viscosity, w_f is fracture width, and Dp is pressure drop between the fracture and the porous rock. Eq. 1 assumes that the average distance that water travels to reach the porous rock is $w_f/2$ —i.e., from the center of the fracture to the fracture face. Consistent with our experimental observations, the gel composition at a given time and point along the fracture was assumed to be uniform across the width of the fracture. In our experiments, the pressure in the porous rock was small (Fig. 6), so Dp in Eq. 1 was close to the actual pressure in the fracture.

As mentioned earlier, after the gel dehydrated, it generally became immobile in the fracture. The mobile gel basically had the same composition as the injected gel. Therefore, at any given time, t , and gel-contacted point along the fracture, the relative gel composition, C/C_o , was estimated using Eq. 2.

$$C/C_o = 1 + \int (2 u_l / w_f) dt \dots\dots\dots (2)$$

A relation was not available between gel composition and gel permeability to water, k_{gel} . Therefore, a simple empirical equation was developed.

$$k_{gel} = 0.11 + (C/C_o)^{-3} \dots\dots\dots (3)$$

In Eq. 3, k_{gel} has units of md when the gel composition, C/C_o , is expressed relative to the composition of our standard Cr(III)-acetate-HPAM gel. Of course, the validity of this empirical equation can be questioned. Eq. 3 was used simply because it allows a reasonable fit for the experimental results. In future studies, a sound relation between gel permeability and composition will be sought experimentally.

Eqs. 1, 2, and 3 were combined with a mass balance to form a simple model of gel propagation and dehydration in

fractures. Based on Fig. 5, pressure gradients in the gel-contacted portions of the fracture were fixed at 28 psi/ft in the first three fracture sections and 50 psi/ft for the last two fracture sections.

Predictions Versus Experimental Results. Leakoff rates predicted by the model are shown in Fig. 14. The model accurately accounted for several experimental observations. First, the model predicted gel arrival at the ends of the first through fifth fracture sections after injecting 0.9, 2.8, 5.7, 10.7, and 16 fracture volumes, respectively. Experimentally, gel actually arrived after 1.1, 2.7, 5.6, 11, and 15 fracture volumes, respectively.

Second, the general shapes of the predicted water leakoff curves (Fig. 14) matched the experimental curves (Fig. 12) reasonably well. The predicted maximum leakoff rate occurred in the first section after injecting 0.9 fracture volumes of gel. For comparison, the experimental maximum in Section 1 was reached after injecting 1.1 fracture volumes. The predicted peak leakoff rates in Sections 2, 3, 4, and 5 were 68%, 54%, 43%, and 35%, respectively, of the predicted peak value in Section 1. The experimental peak leakoff rates in Sections 2, 3, 4, and 5 were 67%, 56%, 53%, and 54%, respectively, of the actual peak leakoff rate.

Third, the model predictions matched the experimental results quite well with regard to the fraction of water flow from the matrix at the core outlet (see Fig. 15).

Fourth, the predicted profiles of final concentrations in the fracture matched the experimental values reasonably well. After 17 fracture volumes of gel injection, the predicted C/C_o values for gel in the fracture ranged from 25 near the fracture inlet to 12 in the fourth fracture section. The experimental values were 20 and 9, respectively (Fig. 9). After 80 fracture volumes of gel injection, the predicted C/C_o values for gel in the fracture ranged from 64 near the fracture inlet to 30 in the fourth fracture section. The experimental values were 36 and 25, respectively (Fig. 9). The model did not account for any entry of free chromium or uncrosslinked polymer into the porous rock. Therefore, the predicted concentrations in the fracture were expected to be somewhat higher than the experimental values.

Relation Between dp/dl and w_f . Earlier, the pressure gradient required for gel extrusion was shown to be inversely proportional to the square of fracture width (Fig. 1 and Eq. 4).

$$dp/dl=0.02/(w_f)^2 \dots\dots\dots(4)$$

Was this behavior expected? For a material with a yield stress, t_y , a simple force balance predicts that the pressure gradient required for extrusion should be given by Eq. 5.

$$dp/dl=2t_y/w_o \dots\dots\dots(5)$$

In this equation, w_o is the effective opening size during extrusion. For our standard one-day-old Cr(III)-acetate-HPAM gel at 41°C, the yield stress was about 0.005 psi (35 Pa). (Jin Liu measured this value using a Paar-Physica Model UDS 200 Universal Dynamic Spectrometer.) For an opening size of 0.04

in. (0.1 cm), Eq. 5 predicts a pressure gradient of 3 psi/ft. In contrast, the experimentally measured values ranged from 28 to 50 psi/ft when the fracture width was 0.04 in.

Why were the experimental pressure gradients much greater than the predicted values? During gel extrusion, recall that the fracture was filled with a concentrated immobile gel. Also recall that only the original gel extruded through the fracture. The original gel must “worm-hole” its way through the concentrated gel. Therefore, the actual opening for gel extrusion, w_o , was generally much less than the fracture width, w_f . Inputting a pressure gradient of 28 psi/ft into Eq. 5 suggests that the actual opening that was available for gel extrusion was about 0.004 in.—one-tenth the fracture width.

The yield stress for a concentrated gel (i.e., taken from a 0.04-in.-wide fracture) was 0.047 psi (325 Pa). Inputting this value into Eq. 5, along with the actual fracture width (0.04 in.) for w_o , gave the pressure gradient measured during gel extrusion (28 psi/ft). This result suggests that the pressure gradient required for extrusion may be determined by a balance between the yield stress of the original (flowing) gel and the yield stress of concentrated gel in the fracture. Additional work will be performed to understand the relation between fracture width and the pressure gradient for gel extrusion.

Future Work

In other future work, using our model and experimental findings, analyses will be performed to predict conditions, gel compositions, and gel volumes that provide the optimum gel placement in fractured reservoirs.

Conclusions

The following conclusions apply to a 1-day-old Cr(III)-acetate-HPAM gel at 41°C:

1. During injection of 80 fracture volumes of the gel, progressive plugging (i.e., continuously increasing pressure gradients) was not observed in any part of a 4-ft-long, 0.04-in.-wide fracture.
2. Effluent from the fracture had the same appearance and a similar composition as those for the injected gel, even though a concentrated, immobile gel formed in the fracture.
3. The concentrated gel formed when water leaked off from the gel along the length of the fracture. The driving force for gel dehydration (and water leakoff) was the pressure difference between the fracture and the adjacent porous rock.
4. During gel extrusion through a fracture of a given width, the pressure gradients and dehydration factors were the same for fractures in 650-md sandstone as in 50-md sandstone and 1.5-md limestone.
5. The gel could extrude through a 28-darcy quartz sandpack, but the average pressure gradient was quite high (~200 psi/ft)—raising concern about the feasibility of extruding this gel through a propped fracture.
6. A simple model was developed that accounted for many of the experimental observations.

Nomenclature

- C = produced concentration, g/m^3
- C_o = injected concentration, g/m^3
- k_f = fracture permeability, darcys [μm^2]
- k_{gel} = gel permeability to water, darcys [μm^2]
- Dp = pressure drop, psi [Pa]
- dp/dl = pressure gradient, psi/ft [Pa/m]
- u_l = water leakoff rate, ft/min [cm/s]
- t = time, s
- w_f = fracture width, in. [m]
- w_o = opening size during extrusion, in. [m]
- m = water viscosity, cp [Pa·s]
- t_y = yield stress, psi [Pa]

Acknowledgments

Financial support for this work is gratefully acknowledged from the United States Department of Energy (NPTO), BDM-Oklahoma, ARCO, British Petroleum, Chevron, China National Petroleum Corp., Chinese Petroleum Corp., Conoco, Exxon, Halliburton, Marathon, Norsk Hydro, Phillips Petroleum, Saga, Schlumberger-Dowell, Shell, Statoil, and Texaco. I thank Richard Schrader for performing the experiments. I also thank Kate Wavrik for determining polymer concentrations and Jin Liu for determining the yield stresses for the gels.

References

1. Sydansk, R.D. and Moore, P.E.: "Gel Conformance Treatments Increase Oil Production in Wyoming," *Oil & Gas J.* (Jan. 20, 1992) 40-45.
2. Borling, D.C.: "Injection Conformance Control Case Histories Using Gels at the Wertz Field CO₂ Tertiary Flood in Wyoming, USA," paper SPE 27825 presented at the 1994 SPE/DOE Symposium on Improved Oil Recovery, April 17-20.
3. Hild, G.P. and Wackowski, R.K.: "Results of the Injection Well Polymer Gel Treatment Program at the Rangely Weber Sand Unit, Rangely, Colorado," paper SPE/DOE 39612 presented at the 1998 SPE/DOE Symposium on Improved Oil Recovery, Tulsa, April 19-22.
4. Lane, R.H. and Sanders, G.S.: "Water Shutoff Through Fullbore Placement of Polymer Gel in Faulted and in Hydraulically Fractured Producers of the Prudhoe Bay Field," paper SPE 29475 presented at the 1995 SPE Production Operations Symposium, Oklahoma City, April 2-4.
5. Seright, R.S.: "Improved Methods for Water Shutoff," Final Technical Progress Report (U.S. DOE Report DOE/PC/91008-14), U.S. DOE Contract DE-AC22-94PC91008, BDM-Oklahoma Subcontract G4S60330 (Oct. 1998) 21-54.
6. Seright, R.S.: "Gel Dehydration During Extrusion Through Fractures," *SPEPF* (May 1999).
7. Seright, R.S.: "Gel Placement in Fractured Systems," *SPEPF* (Nov. 1995), 241-248.
8. Seright, R.S.: "Use of Preformed Gels for Conformance Control in Fractured Systems," *SPEPF* (Feb. 1997) 59-65.
9. Seright, R.S.: "Effect of Rock Permeability on Gel Performance in Fluid-Diversion Applications," *In Situ* (1993) 17, No. 4, 363-386.

SI Metric Conversion Factors

- cp x 1.0* E-03 = Pa·s
- ft x 3.048* E-01 = m
- in. x 2.54* E+00 = cm
- md x 9.869 233 E-04 = μm^2
- psi x 6.894 757 E+00 = kPa

*Conversion is exact.

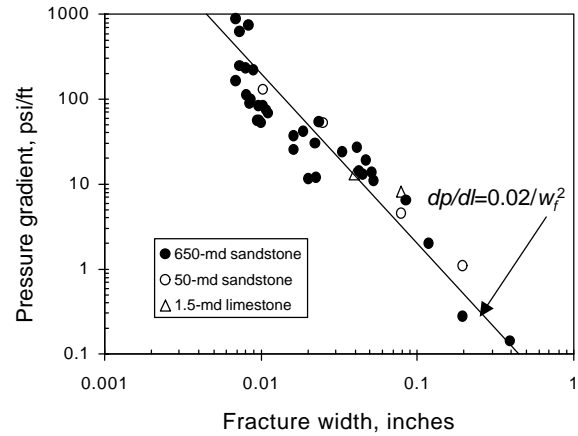


Fig. 1—Pressure gradients required to extrude a one-day-old Cr(III)-acetate-HPAM gel through open fractures (no proppant).

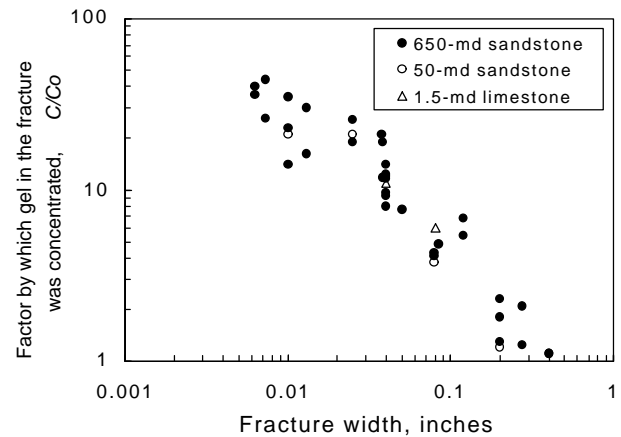


Fig. 2—Degree of gel dehydration versus fracture width.

Core dimensions: 48" x 1.5" x 1.5"
 Core material: 650-md Berea sandstone.
 Fracture $k_f w_f = 277$ darcy-ft. $w_f = 0.04"$.

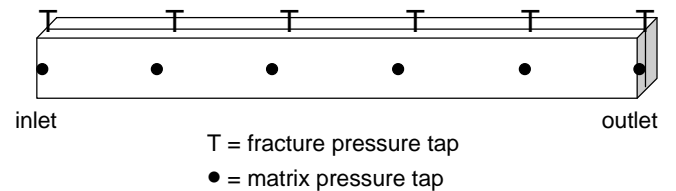


Fig. 3—Illustration of the fractured core.

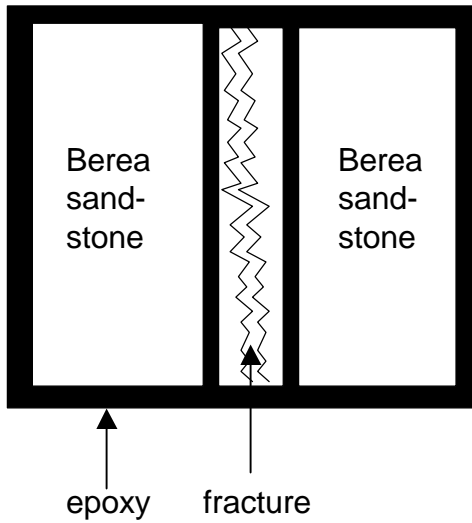


Fig. 4—Core outlet configuration to separate fracture effluent from porous-rock effluent.

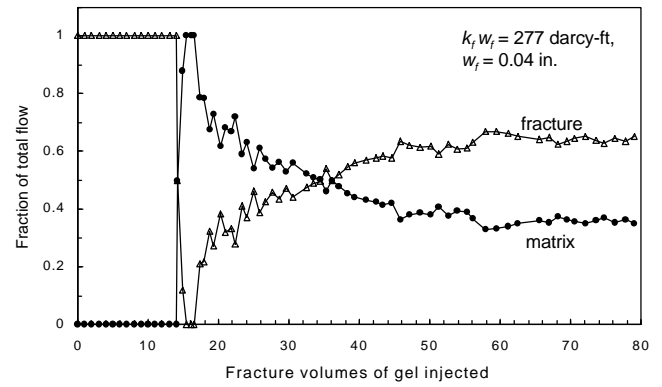


Fig. 7—Fractional flow measured at the core outlet.

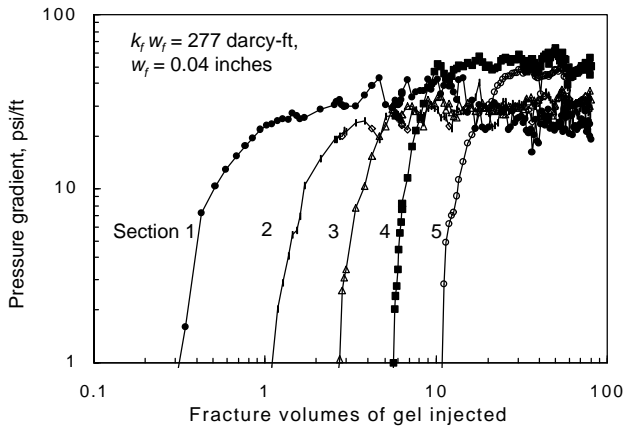


Fig. 5—Pressure behavior in the fracture taps during gel injection.

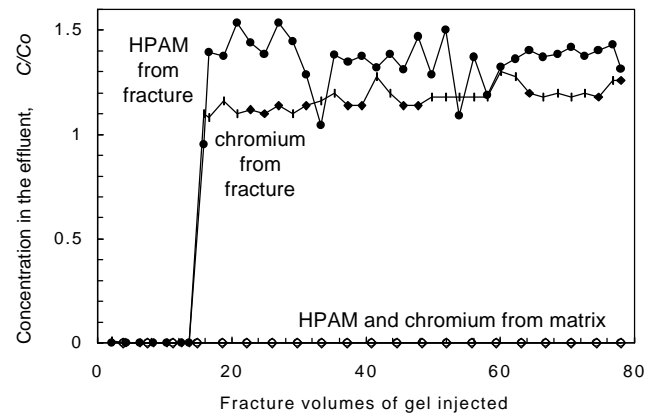


Fig. 8—Chromium and HPAM concentrations in the effluent: fracture versus matrix.

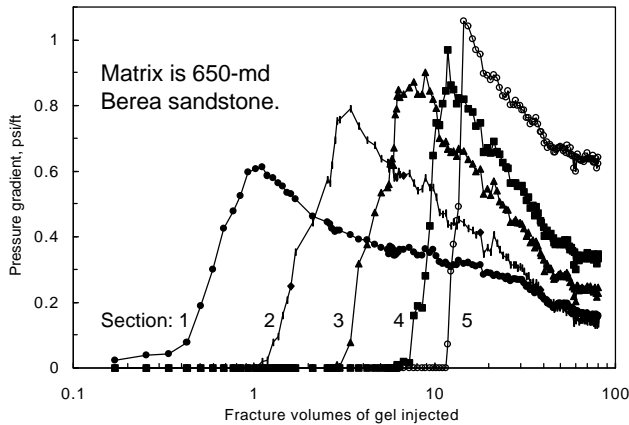


Fig. 6—Pressure behavior in the matrix taps during gel injection.

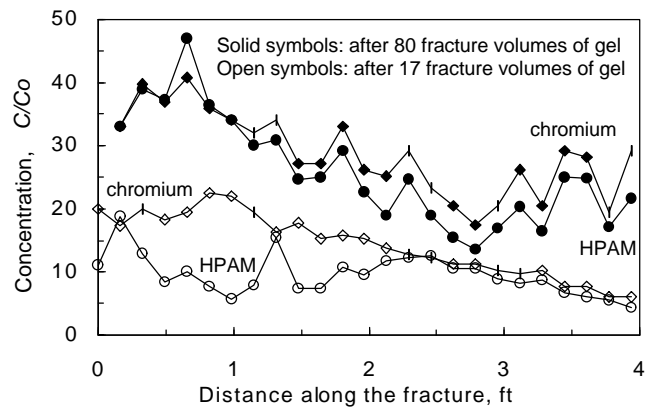


Fig. 9—Composition of gel in the fracture (relative to the injected gel).

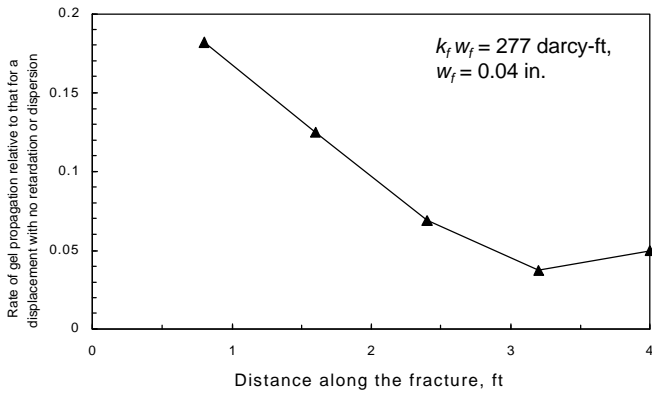


Fig. 10—Gel propagation rate in the fracture.

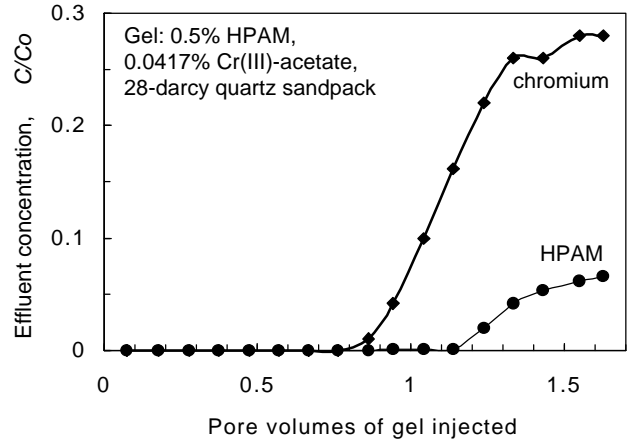


Fig. 13—Composition of the sandpack effluent.

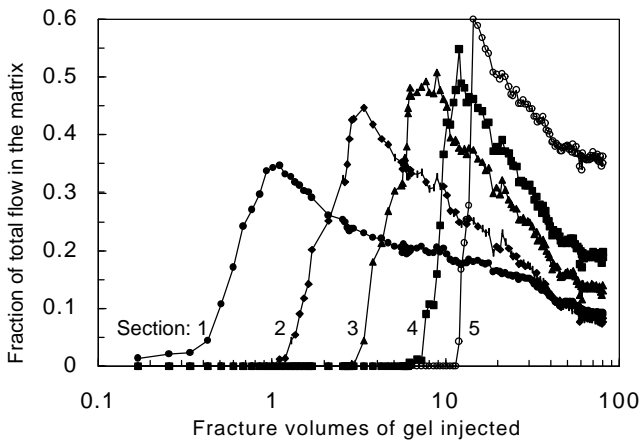


Fig. 11—Brine flow in the porous rock during gel injection.

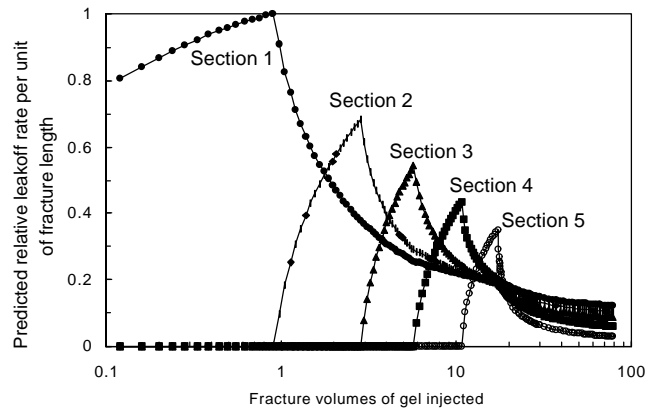


Fig. 14—Predicted leakoff rates.

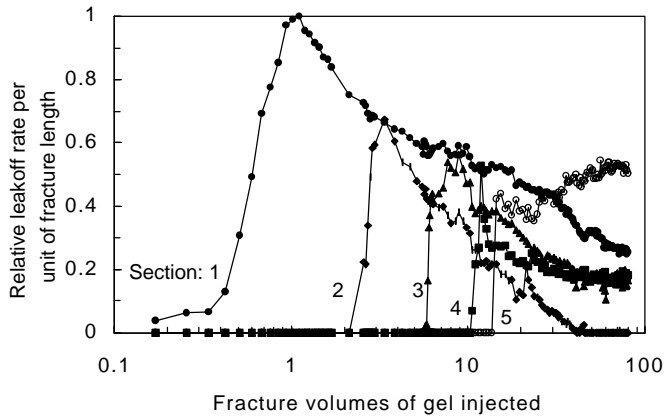


Fig. 12—Relative leakoff rates derived from Fig. 11.

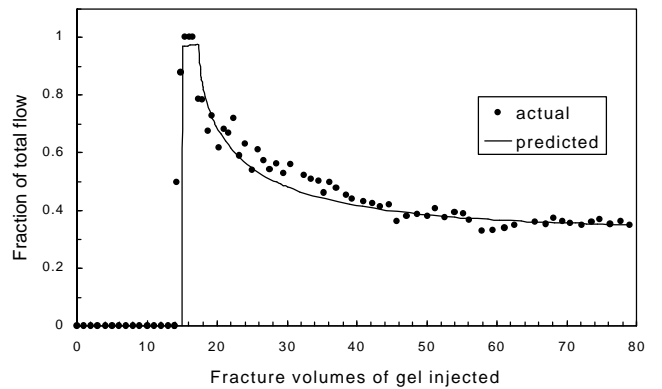


Fig. 15—Predicted versus actual fractional flow from the matrix at the core outlet.